

The Effect of the Cadmium Chloride Treatment on RF Sputtered $\text{Cd}_{0.6}\text{Zn}_{0.4}\text{Te}$ Films for Application in Multi-junction Solar Cells

Running title: Effect of Cadmium Chloride Treatment on Cadmium Zinc Telluride Films

Running Authors: Shimpi et al.

Tushar M. Shimpi^{a)}, Jason M. Kephart, Drew E. Swanson, Amit H. Munshi and
Walajabad S. Sampath

Department of Mechanical Engineering, Colorado State University, 1320 Campus Delivery, Fort Collins, Colorado 80523

A. Abbas, and John M. Walls

CREST (Centre for Renewable Energy Systems and Technology), Loughborough University, Loughborough, LE11 3TU, United Kingdom

^{a)} Electronic mail: mechanical.tushar@gmail.com

Single phase $\text{Cd}_{0.6}\text{Zn}_{0.4}\text{Te}$ (CdZnTe) films, 1 μm thick, were deposited by RF planar magnetron sputter deposition on commercial soda lime glass samples coated with fluorine-doped tin oxide and cadmium sulphide (CdS). The stack was then treated with Cadmium Chloride (CdCl_2) at different temperatures using a constant treatment time. The effect of the CdCl_2 treatment was studied using optical, materials, and electrical characterization of the samples and compared with the as-deposited CdZnTe film with the same stack configuration. The band gap deduced from Tauc plots on the as-deposited CdZnTe thin film was 1.72 eV. The deposited film had good crystalline quality with a preferred orientation along the $\{111\}$ plane. After the CdCl_2 treatment, the absorption edge shifted towards longer wavelength region and new peaks corresponding to cadmium telluride (CdTe) emerged in the X-ray diffraction pattern. This suggested loss of zinc after the CdCl_2 treatment. The cross sectional transmission electron microscope images of

the sample treated at 400°C and the energy dispersive elemental maps revealed the absence of chlorine along the grain boundaries of CdZnTe and residual CdTe. The presence of chlorine in CdTe devices plays a vital role in drastically improving the device performance which was not observed in CdZnTe samples treated with CdCl₂. The loss of zinc from the surface and incomplete recrystallization of the grains together with the presence of high densities of stacking faults were observed. The surface images using scanning electron microscopy showed that the morphology of the grains changed from small spherical shape to large grains formed due to the fusion of small grains with distinct grain boundaries visible at the higher CdCl₂ treatment temperatures. The absence of chlorine along the grain boundaries, incomplete recrystallization and distinct grain boundaries is understood to cause the poor performance of the fabricated devices.

I. INTRODUCTION

To utilize the photons from sun's spectrum efficiently, minimize thermalization losses, and increase efficiency, a multijunction solar cell is a promising alternative to a single junction solar cell. Numerical simulations based on the daily energy densities indicate that the optimum band gap for the top cell absorber should be around ~1.72 eV in a two junction solar cell¹. CdZnTe alloy has the zinc blende structure which is the same as that of CdTe^{2,3} and is a potential candidate for the top cell absorber in a multijunction solar cell. Based on the zinc composition, the band gap of the alloy can be varied from 1.48 eV to 2.26 eV⁴. Using interpolation, a band gap of 1.72 eV can be obtained by using 40% zinc telluride composition in the CdZnTe alloy⁵.

Deposition methods such as Metal Organic Chemical Vapor Deposition (MOCVD)^{5,6}, Vapor Transport⁷, Close Space Sublimation(CSS)⁸ and co-sputtering of

CdTe and ZnTe⁹ have been used to deposit CdZnTe thin films with different compositions by various research groups. The loss of zinc during the CdCl₂ activation treatment from the deposited CdZnTe films has been extensively reported^{4,6,8}. However, the devices fabricated after CdCl₂ treatment, exhibited low photo generated current and very low fill factor. This leads to a low device performance irrespective of the deposition method used. If the CdCl₂ treatment is carried out at higher temperatures (in excess of 400°C)^{7,10}, an improvement in the device performance is observed. The improvement is associated with almost complete loss of zinc which reduces the band gap of the CdZnTe material to that of the lower band gap CdTe material. However, this improvement is disadvantageous since a higher band gap material is required for the fabrication of the top cell.

The cadmium chloride activation treatment of CdTe films is a critical step in improving the device performance of CdTe absorber based solar cells. The CdCl₂ treatment of thin film CdTe has been broadly studied and frequently reported in the literature¹¹⁻¹⁶. During the CdCl₂ treatment, chlorine is introduced into the CdTe using various techniques such as a vapor treatment¹⁷ or by the application of CdCl₂ solution and then annealing at approximately 400°C¹⁵. The improvement in the device performance is caused by the presence of chlorine along the grain boundaries of CdTe^{11,12} and is attributed to recrystallization¹³⁻¹⁵, grain growth, removal of stacking faults¹⁷ and doping of grain boundaries n-type within the p-type CdTe absorber¹¹. For CdZnTe devices, there is a lack of reports on understanding regarding the incorporation of chlorine in the bulk of the CdZnTe and in the residual CdTe, microstructural changes in the material, the status of stacking faults and recrystallization after the CdCl₂ treatment. In this work, the CdCl₂

treatment was performed on $\text{Cd}_{0.6}\text{Zn}_{0.4}\text{Te}$ films deposited by RF sputtering on CdS. Optical, material, and electrical characterizations were conducted to understand the changes caused to the CdZnTe film microstructure, the presence and distribution of chlorine together with the effect on the existence of stacking faults and other recrystallization processes caused by the CdCl_2 treatment.

II. EXPERIMENTAL DETAILS

For this study, samples were fabricated and characterized on TEC12D glass (Nippon Sheet Glass Co., Ltd). This glass has a coating of fluorine doped tin oxide on one side which serves as the transparent conducting oxide (TCO). The substrates were cleaned ultrasonically for 30 minutes in deionized water before deposition. Plasma cleaning at 400V, 15mA in an Ar/O₂ atmosphere was carried out individually on each sample¹⁸. After plasma cleaning, without breaking the vacuum, samples were transferred to a heater station for heating the substrate. The top and bottom heaters were maintained at 620°C and the heating time was 110 seconds. The average temperature of the sample after heating was measured with a pyrometer and was about 480°C. Cadmium sulphide (CdS) was deposited using close space sublimation (CSS) process on the fluorine doped tin oxide side of the sample. The temperature of the CdS source was 620°C and the deposited film thickness was 125 nm. The details of deposition and a description of the vacuum system is provided elsewhere¹⁹. The samples were then cooled to room temperature and after breaking the vacuum, the cadmium zinc telluride (CdZnTe) sputter-deposition was carried out in a separate chamber.

Prior to the RF sputter-deposition, the chamber was pumped down to a base pressure of 10^{-5} Torr. To minimize residual oxygen, the chamber was purged several

times with Ar gas. The samples coated with CdS were baked for 15 minutes once the heaters reached the process temperature. The CdZnTe films were deposited using a single target with a composition of CdTe (60 wt%) and ZnTe (40 wt%) fabricated by Plasmaterials Inc. The CdZnTe target was plasma cleaned for 3 minutes with the shutter closed to prevent deposition. The deposition details of the RF sputtering process for CdZnTe are provided in table 1.

Table. 1. Deposition process details for CdZnTe films

<i>RF Power</i>	60W	<i>Process Gas and Press.</i>	Ar, 10mTorr
<i>Dep. Time</i>	36 minutes	<i>Thickness</i>	~1 micron
<i>Dep. Temp.</i>	400C	<i>Distance substrate to target</i>	10 cm

The cadmium chloride (CdCl_2) treatment was carried in a horizontal CSS system (Figure 1). Approximately 10 g of CdCl_2 material (99.99% pure) was placed in the graphite boat. For the treatment, each sample was placed over the graphite boat and heated using infra-red (IR) lamps. A thermocouple attached to the graphite boat and the top plate recorded the process temperatures. The process gas used was Ar and the process pressure was ~10Torr. Two samples were treated at different temperatures (380°C and 400°C) for 3 minutes and one sample was retained untreated as a control. Other process conditions for the treatment of the two samples were maintained the same.

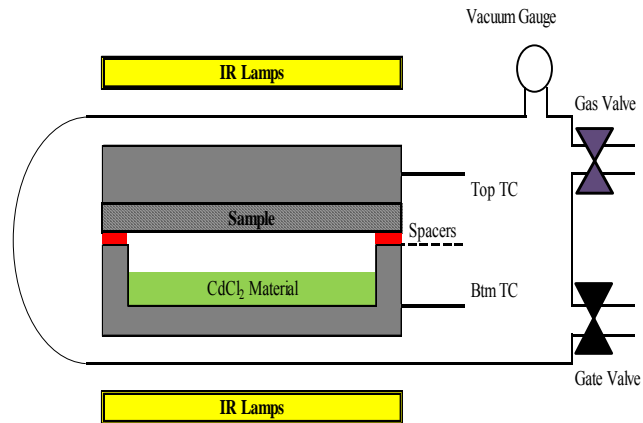


Fig. 1. A schematic of horizontal bell jar used for CdCl₂ activation treatment

After the CdCl₂ treatment, the samples were cut into two halves. On one half, optical transmission and material characterization measurements were conducted. For materials characterization, X-ray diffraction (XRD), Scanning Electron Microscopy (SEM) and Transmission Electron Microscopy (TEM) analyses were performed. On the other half, devices were fabricated after copper doping, and carbon and nickel paints were applied as a back electrode. Current-voltage (JV) measurements on the devices were carried out under AM 1.5 conditions using an ABET Technologies solar simulator.

Transmission was measured from 350 to 1000 nm was using Ocean Optics Inc. hardware coupled with LabVIEW software. The Bruker AXS D8 system was used to conduct X ray diffraction measurements. The wavelength of Cu K_{α1} radiation was 1.54046 Å and the diffracted signal was collected on scintillating counter. Surface images were obtained at 15 KV using a JEOL JSM 6500F scanning electron microscope. Sample cross sections for transmission electron microscopy (TEM) were prepared using a focused ion beam (FIB) with a dual beam FEI Nova 600 Nanolab. A JEOL 2000FX transmission electron microscope was used to obtain the TEM images.

III. RESULTS AND DISCUSSION

A. Transmission Measurements

Light passing through the fluorine doped tin oxide film was used as a 100% baseline. Transmission was measured at the same location on all three samples and is shown in figure 2.

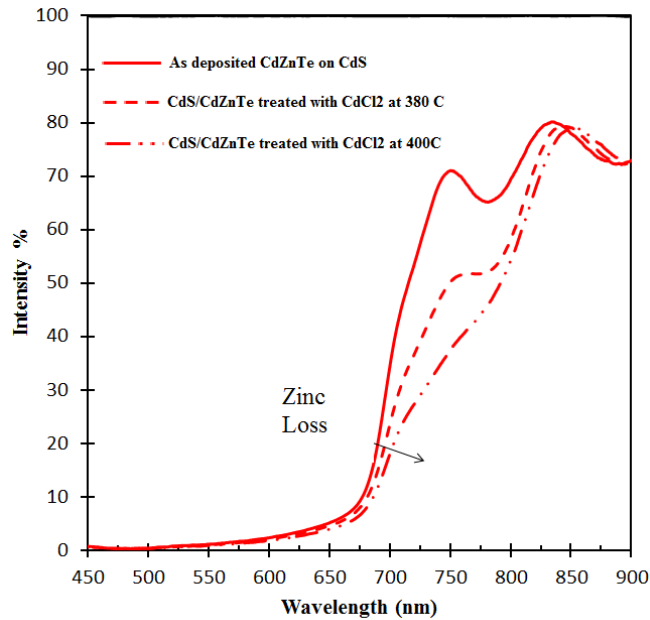


Fig. 2. Transmission spectra of CdZnTe samples treated with CdCl₂ at different temperatures and compared with the as-deposited.

On the as-deposited CdZnTe sample, the transmittance was below 5% till 650 nm and above 60% in the long wavelength region which makes the material suitable for use as a top cell in a multijunction solar cell. The absorption edge of the as-deposited CdZnTe film was near vertical confirming the good crystalline quality of the film. The band gap calculated using the Tauc plot method was 1.72 eV. The influence of the CdCl₂ treatment can be observed on the absorption edges of the treated samples. The edges are

less distinct and shifted towards the longer wavelength region. This is a clear indication of some loss of zinc from the CdZnTe films treated with CdCl₂.

B. X Ray Diffraction

To understand the compositional changes in the CdZnTe films after the CdCl₂ treatment, XRD was conducted by using a Bragg-Brentano configuration. The angle was scanned from 10° to 80° with a step size of 0.05°. The obtained peaks were compared to ICDD cards of CdTe (00-015-0770), ZnTe (00-015-0746) and various compositions of CdZnTe (00-050-1439 Cd_{0.6}Zn_{0.4}Te, 00-053-0553 Cd_{0.45}Zn_{0.55}Te, 00-053-0552 Cd_{0.85}Zn_{0.15}Te). To identify and eliminate peaks from fluorine doped tin oxide and CdS, XRD was also carried out on a sample with CdS deposited on TEC12D glass. The diffraction patterns from all these measurements are shown in figure 3.

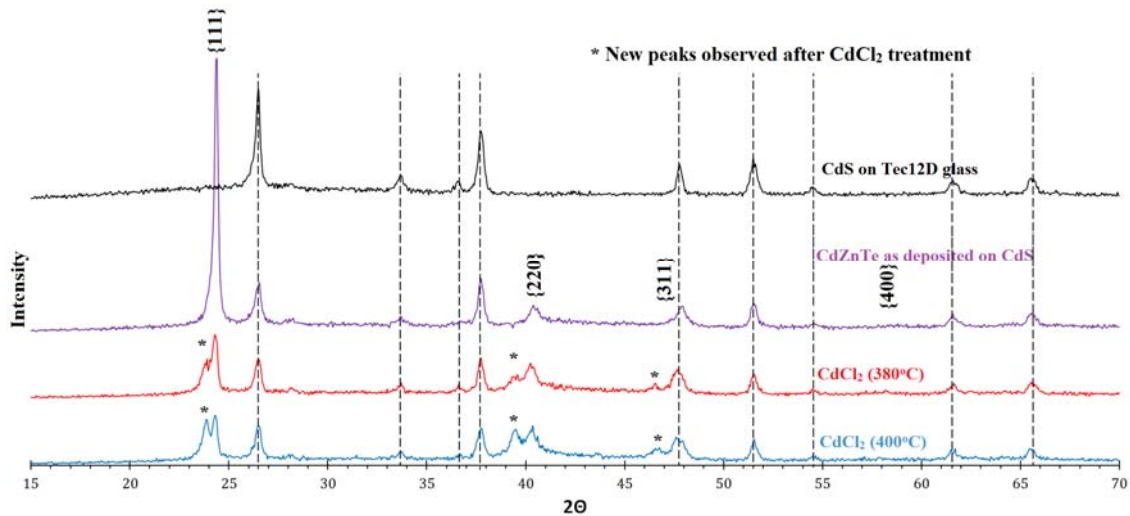


Fig. 3. X ray diffraction spectra from CdZnTe samples treated with CdCl₂ at different temperatures and compared with as-deposited CdZnTe and CdS deposited on TEC12D glass

The vertical dashed lines eliminate the peaks from fluorine doped tin oxide and CdS. The as-deposited CdZnTe film had a preferred orientation along the {111} plane

with a peak at $2\theta = 24.28^\circ$. The other peaks at 40.17° , 47.56° and 58.15° relating to the $\{220\}$, $\{311\}$ and $\{400\}$ planes had a very low intensity. The composition of the as-deposited film was close to the $\text{Cd}_{0.6}\text{Zn}_{0.4}\text{Te}$ alloy when compared to the ICDD card. No peaks from CdTe or ZnTe were detected suggesting that there was no preferential sputtering from the target and the deposited film was single phase. In the diffraction spectrum of the sample treated with CdCl_2 at 380°C , a shoulder appeared to the left of the $\{111\}$ peak and transformed to a separate peak at $2\theta = \sim 23.8^\circ$ with the CdCl_2 treatment at 400°C . The interplanar spacing and lattice parameter was calculated for the new peaks and substituted in Vegard's equation⁵. The composition of the compound was found to be close to CdTe. This suggests that both CdZnTe and CdTe compounds exist after the CdCl_2 treatment.

C. Transmission Electron Microscopy

To locate the zinc loss from CdZnTe and to identify microstructural changes, a cross sectional specimen of CdZnTe treated with CdCl_2 at 400°C was prepared using the focused ion beam specimen technique using a standard in-situ lift out method. The cross section was examined using TEM (figure 4) and Energy Dispersive X-ray (EDX) elemental mapping was carried out (figure 5) on the same cross section.

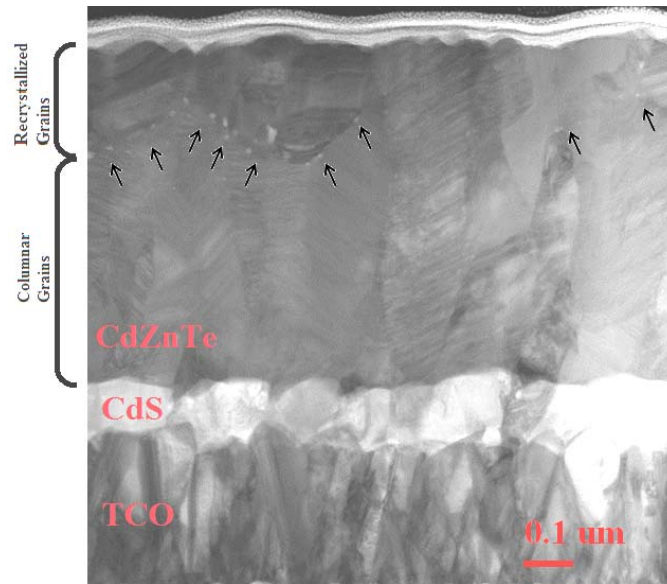


Fig. 4. TEM image of a cross section of CdS/CdZnTe treated with CdCl₂ at 400°C. Arrows pointing towards the voids observed at the interface between the recrystallized and columnar grains.

In the TEM image of the cross section, the effect of CdCl₂ can be observed near the surface of CdZnTe films. It appears that the recrystallization starts at the surface and proceeds towards the junction of the CdS/CdZnTe. The recrystallization is incomplete. This is different to the process observed in sputtered CdTe treated with CdCl₂¹⁵. The morphology of the grains near the surface changed from a columnar grain shape to an oval shape. Stress during the grain growth induces the formation of voids which are observed near grain boundaries of recrystallized grains. Below the recrystallized grains, the columnar grains are observed which are the characteristic of sputter-deposited films are observed. In the columnar grains, the presence of a high density of stacking faults can be observed in the image.

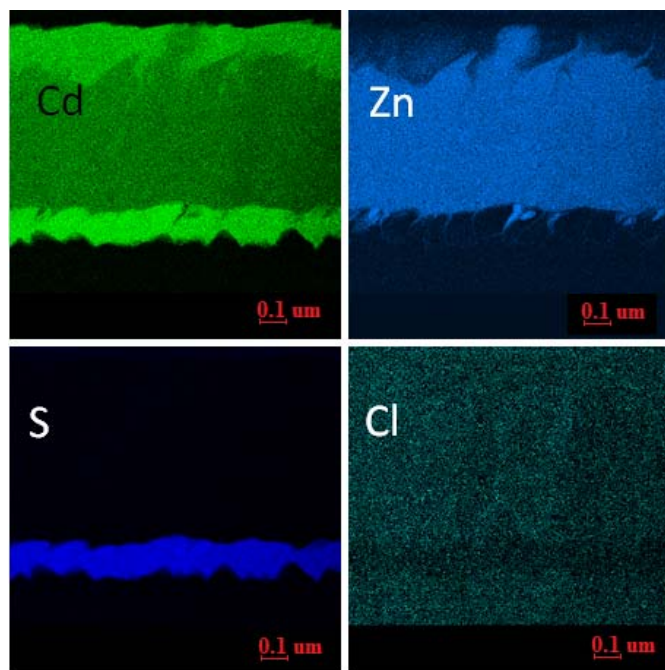


Fig. 5. Elemental maps collected from the cross section of the sample treated with CdCl₂ at 400°C. Individual elemental maps are labelled with the elemental symbol.

In the EDX elemental maps shown in figure 5, the zinc loss from the surface region is confirmed. The CdCl₂ vapors react with zinc in the CdZnTe layer and forms ZnCl₂⁶. At the treatment temperatures, ZnCl₂ has a higher vapor pressure than CdCl₂ and CdTe which causes zinc and chlorine to evaporate from the CdZnTe layer. At the junction of CdS/CdZnTe, zinc diffusion into the CdS can also be observed. This would probably lead to the formation of Cd_(1-x)Zn_xS or ZnS compound in very small concentrations at the junction. Due to the low concentration, no diffracted peak signal corresponding to the Cd_(1-x)Zn_xS or ZnS compound was detected in the XRD measurements. The critical observation was that the chlorine signal was below the detection limit of EDX in the zinc depleted region, along the grain boundaries of CdZnTe and at the junction of CdS/CdZnTe. In typical CdTe devices, optimal CdCl₂ treatment results in the decoration of grain boundaries with CdCl₂ that is clearly observed in the

TEM¹⁷. In the zinc depleted region of the sample, the residual compound is CdTe and there is no strong signal from chlorine. This indicates that the CdTe which has been formed after the CdCl₂ treatment is subsequently recrystallized but there is absence of chlorine at the grain boundaries. It has been shown that stacking faults are present, if there is no chlorine present at the grain boundaries¹⁷. The absence of a discernible chlorine signal along the grain boundaries of the CdZnTe and at the junction of CdS/CdZnTe suggests that the material present in these regions is unchanged from the as-deposited and is highly defective.

D. Scanning Electron Microscopy

SEM images from the surface of the samples are shown in figure 6.

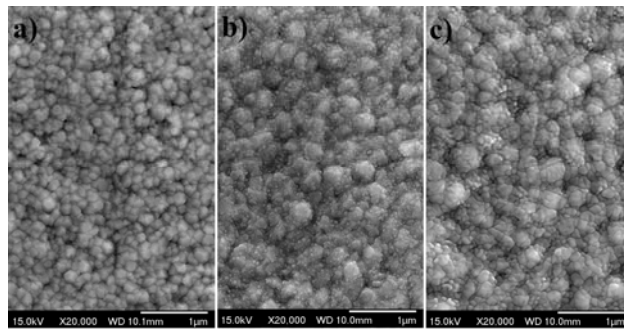


Fig. 6. SEM images a) As-deposited CdZnTe, b) CdZnTe treated with CdCl₂ at 380°C and c) CdZnTe treated with CdCl₂ at 400°C

The grains are spherically shaped and uniform on the as-deposited CdZnTe sample. Recrystallization, grain coalescence and enlargement are observed in the CdCl₂ treated samples. In the sample treated with CdCl₂ at 380°C, spherical shaped grains and newly formed larger grains are observed. At the higher CdCl₂ treatment temperature, large grains are formed by the fusion of small grains with distinct grain boundaries. It has been reported that after CdCl₂ treatment on CdTe, grains coalesce and grain boundaries

are hard to distinguish under SEM. Such effects were not observed in the CdCl₂ treated CdZnTe.

E. Photovoltaic Performance

The current voltage measurements were carried out on all the devices under AM 1.5 illumination. The voltage was swept from -0.8 V to 1.2 V. The performance parameters obtained are listed in table 2.

Table 2. Current voltage graph parameters

<i>Sample description</i>	<i>Open circuit voltage (mV)</i>	<i>Short circuit current density (mA/cm²)</i>	<i>Fill Factor</i>
<i>As-deposited CdZnTe</i>	260	0.75	28
<i>CdCl₂ treated CdZnTe at 380°C</i>	447	1.8	27
<i>CdCl₂ treated CdZnTe at 400°C</i>	524	2.8	30.5

For a material with a band gap of 1.72 eV, the theoretical open circuit voltage and short circuit current density should be ~ 1.4V and ~ 20mA/cm²²⁰. The open circuit voltage, short circuit current density and fill factor values of all the three samples are substantially below these theoretical values. There is an improvement in the open circuit voltage as the CdCl₂ treatment temperature increases and a very slight improvement in the short circuit current density and fill factor. This is probably due to the presence of more distinct grain boundaries. These grain boundaries are not being doped with chlorine

along with incomplete recrystallization and the existence of stacking faults which would act as recombination centers.

IV. SUMMARY AND CONCLUSIONS

The effect of the CdCl₂ treatment was studied on the stack comprising of TEC12D/CdS/CdZnTe by varying the treatment temperature. The as-deposited CdZnTe was a single phase with a preferred orientation along the {111} plane and had a band gap of 1.72 eV. Surface images showed that the grains were spherically shaped and uniformly distributed over the surface. After the CdCl₂ treatment at various temperatures, the absorption edge moved towards the higher wavelength region which is an indication of zinc loss and resulted in a reduced band gap of the material. XRD confirmed that CdZnTe was no longer a single uniform composition after the treatment as peaks corresponding to CdTe were identifiable. There was more loss of zinc with increased treatment temperature. Important insights were obtained from TEM images and EDS elemental maps of the sample treated at 400°C which showed the absence of chlorine along the grain boundaries of CdZnTe and residual CdTe after zinc loss. Recrystallization and grain growth were observed at the surface of the CdZnTe and it appeared that grain growth started at the surface and proceeded towards the junction of CdS/CdZnTe. High densities of stacking faults were present in the columnar grains below the recrystallized region. The SEM images showed that the grain boundaries were distinct. The absence of chlorine along the grain boundaries of CdZnTe and residual CdTe, incomplete recrystallization and presence of stacking faults were considered responsible for the poor performance in the fabricated devices.

ACKNOWLEDGMENTS

This work was supported by National Science Foundation-Industrial/ University Center of Research and Cooperation for Next Generation Photovoltaics group and the authors would like to express gratitude. The authors would like to thank James Sites, Kurt Barth and Jennifer Drayton for their insights and suggestions on the work during the lab meetings. Special thanks to Kevan Cameron, Carey Reich, Cristina Moffett and Marina D'Ambrosio for their assistance in the PV manufacturing lab.

- ¹T. J. Coutts, J. S. Ward, D. L. Young, K. A. Emery, T. A. Gessert, and R. Noufi, *Prog. Photovoltaics Res. Appl.*, **11**, 359 (2003).
- ²J.-H. Yang, S. Chen, W.-J. Yin, X. G. Gong, A. Walsh, and S.-H. Wei, *Phys. Rev. B*, **79**, 245202 (2009).
- ³K. S. Rahman, F. Haque, N. A. Khan, M. A. Islam, M. M. Alam, Z. A. Alothman, K. Sopian, and N. Amin, *Chalcogenide Lett.*, **11**, 129 (2014).
- ⁴B. E. McCandless, "Cadmium Zinc Telluride Films for Wide Band Gap Solar Cells" in *29th IEEE PVSC* (2002).
- ⁵S. . A. Ringel, R. Sudharsanan, A. Rohatgi, and W. B. Carter, *J. Electron. Mater.*, **19**, 259 (1989).
- ⁶A. Rohatgi, R. Sudharsanan, S. Ringel, and M. MacDougal, *Sol. Cells*, **30**, 109 (1991).
- ⁷B. E. Mccandless, W. A. Buchanan, and G. M. Hanket, "Thin Film Cadmium Zinc Telluride Solar Cells" in *4th IEEE World Conf.on Photovoltaic Energy Conversion* (2006).
- ⁸R. Dhere, T. Gessert, J. Zhou, S. Asher, J. Pankow, and H. Moutinho, *MRS Proc.***763** (2003).
- ⁹J. Gaduputi, "Characterization Of Cadmium Zinc Telluride Films And Solar Cells On Glass And Flexible Substrates By RF Sputtering," *University of South Florida* (2004).

- ¹⁰S. H. Lee, A. Gupta, and A. D. Compaan, *Phys. Status Solidi*, **1**, 1042 (2004).
- ¹¹C. Li, Y. Wu, J. Poplawsky, T. J. Pennycook, N. Paudel, W. Yin, S. J. Haigh, M. P. Oxley, A. R. Lupini, M. Al-Jassim, S. J. Pennycook, and Y. Yan, *Phys. Rev. Lett.*, **112**, 156103 (2014).
- ¹²M. Terheggen, H. Heinrich, G. Kostorz, A. Romeo, D. Baetzner, A. N. Tiwari, A. Bosio, and N. Romeo, *Thin Solid Films*, **431**, 262 (2003).
- ¹³B. E. McCandless, L. V. Moulton, and R. W. Birkmire, *Prog. Photovoltaics Res. Appl.*, **5**, 249 (1997).
- ¹⁴M. Rami, E. Benamar, M. Fahoume, F. Chraïbi, and A. Ennaoui, *M. J. Condensed Matter*, **3**, 66 (2000).
- ¹⁵A. Abbas, B. Maniscalco, J. W. Bowers, P. M. Kaminski, G. D. West, and J. M. Walls, “Initiation of the Cadmium Chloride Assisted Re-Crystallization Process of Magnetron Sputtered Thin Film CdTe” in *Conf. Rec. IEEE Photovolt. Spec.*, (2013).
- ¹⁶J. Lee, *Curr. Appl. Phys.*, **11**, 103 (2011).
- ¹⁷A. Abbas, G. D. West, J. W. Bowers, P. Isherwood, P. M. Kaminski, B. Maniscalco, P. Rowley, J. M. Walls, K. Barricklow, W. S. Sampath, and K. L. Barth, *IEEE J. Photovoltaics*, **3**, 1361 (2013).
- ¹⁸D. E. Swanson, R. Geisthardt, J. T. Mc Goffin, J. D. Williams, and J. R. Sites, *IEEE J. Photovoltaics*, **3**, 838 (2013).
- ¹⁹D. E. Swanson, J. M. Kephart, P. S. Kobayakov, K. Walters, K. C. Cameron, K. L. Barth, W. S. Sampath, J. Drayton, and J. R. Sites, *J. Vac. Sci. Technol. A Vacuum, Surfaces, Film.*, **34**, 021202 (2016).
- ²⁰F. Meillaud, A. Shah, C. Droz, E. Vallat-Sauvain, and C. Miazza, *Sol. Energy Mater. Sol. Cells*, **90**, 2952 (2006).